Received 16 April 2024; revised 31 May 2024; accepted 21 July 2024. Date of publication 22 July 2024; date of current version 5 August 2024.
The review of this article was arranged by Editor S. Reggiani.

Digital Object Identifier 10.1109/JEDS.2024.3432783

Vertical GaN Schottky Barrier Diode With Hybrid P-NiO Junction Termination Extension

SHAOCHENG LI [1] (Graduate Student Member, IEEE), SHU YANG [2] (Senior Member, IEEE), ZHAO HAN [2] (Graduate Student Member, IEEE), WEIBING HAO [2] (Member, IEEE), KUANG SHENG [1] (Senior Member, IEEE), GUANGWEI XU [2] (Member, IEEE), AND SHIBING LONG [2] (Senior Member, IEEE)

1 College of Electrical Engineering, Zhejiang University, Hangzhou 310027, China
2 School of Microelectronics, University of Science and Technology of China, Hefei 230026, China

CORRESPONDING AUTHOR: S. YANG (e-mail: eesyang@ustc.edu.cn)

This work was supported in part by the National Key Research and Development Program of China under Grant 2023YFB3611902; in part by the National Natural Science Foundation of China (NSFC) under Grant 52077200, Grant 61925110, and Grant 62334012; and in part by the Power Electronics Science and Education Development Program of Delta Group under Grant DREK2022001.

ABSTRACT Selective-area p-type doping has been regarded as one of the primary challenges in vertical GaN junction-based power devices. Nickel oxide (NiO), serving as a natural p-type semiconductor without the requirement for sophisticated activation and enabling adjustable charge concentration, is potentially feasible to form pn hetero-junction in GaN power devices. In this work, a vertical GaN Schottky barrier diode (SBD) featuring hybrid p-NiO junction termination extension (HP-JTE) with fluorine (F)-implanted buried layer (FIBL) has been demonstrated. With FIBL incorporated underneath p-NiO in the termination region, the reverse leakage current can be effectively reduced by approximately 3 orders of magnitude. By virtue of photon emission microscopy measurements, it has also been verified that the light emission and leakage current through p-NiO termination region can be effectively suppressed by FIBL. Thanks to the HP-JTE structure as well as the nearly ideal Schottky interface, the vertical GaN SBD exhibits a high current swing of $\sim 10^{13}$, a low ideality factor of ~1.02, a low differential R_{ON} of ~0.89 m$\Omega \cdot$cm^2, a low forward voltage drop of ~ 0.8 V(defined at 100 A/cm^2), and a breakdown voltage of ~ 780 V(defined at 0.1 A/cm^2). The characterizations and findings in this work can provide valuable insights into the p-NiO/GaN hetero-junction-based power devices.

INDEX TERMS GaN, junction termination extension, leakage current, NiO, SBD.

I. INTRODUCTION

Gallium nitride (GaN)-based power devices, featuring low power losses and high switching frequency, have been used in building compact and light-weight power electronic systems with increased power density and enhanced energy efficiency [1], [2]. Owing to the emergence of high-quality commercial free-standing GaN substrates up to 6-inch [3], the vertical GaN-on-GaN power devices, which can achieve high Baliga's figure-of-merit (BFOM) [4], [5], [6], [7], [8] and superior dynamic R_{ON} performance [9] have shown great potential for next-generation power electronic applications.

In general, selective-area p-type doping technique plays an important role in vertical power devices, where the p-type region can modulate the electrical field in active or termination regions [10], [11], [12], [13], [14], [15], [16]. However, formation of selective-area p-type region in GaN is confronted with challenges as follows: (1) The activation of Magnesium (Mg) ion implantation in GaN usually requires sophisticated annealing at high temperature (≥1200 °C) and ultra-high pressure (≥1 GPa) atmosphere to prevent the possible decomposition of GaN surface at high temperature [17], [18], [19], [20]. (2) Selective-area p-GaN regrowth technique usually suffers from relatively high leakage current, which is possibly caused by impurities/etching damages at the regrown interface [21], [22], [23], [24], [25].

Nickel oxide (NiO) with a wide bandgap (3.4∼4 eV) and a relatively small lattice mismatch (∼8%) with GaN [26], [27], [28], is a natural p-type semiconductor without the requirement of sophisticated activation process [29]. A wide range of hole concentration (10^{15} cm^{-3} ∼10^{20} cm^{-3}) can be achieved in NiO by adjusting O_2/N_2 flow ratio during NiO deposition [30], [31], [32]. Therefore, NiO is potentially feasible to form pn heterojunction (HJ) in GaN power electronic devices including E-mode lateral HEMTs [33], [34], vertical Schottky barrier diodes (SBDs) [30], [35], [36], [37] vertical HJ diodes [30], [32], [37] and super-junction diodes [27].

The electric field crowding effect at the junction edge limits the breakdown voltage of GaN SBDs. Thanks to the electric field modulation by p-NiO, it has been reported that the breakdown voltage of GaN quasi-vertical SBDs with etched-mesa edge termination have been enhanced by covering the mesa sidewall with p-NiO [35] or combining planar p-NiO with field plate structure [36]. However, it has been widely observed that the leakage current would increase by several orders of magnitude with the incorporation of p-NiO into GaN SBDs with only planar p-NiO JTE [30], [37], [38] and NiO/GaN HJ diodes [30], [32], [37]. Hence, it is essentially important to develop effective approaches for suppressing p-NiO-induced leakage current. Due to the strong electronegativity [39], [40], fluorine (F) ion implantation can be utilized to form fully-depleted region in n-GaN, aiming at suppressing the reverse leakage current in GaN diodes [41], [42], [43], [44] and GaN HEMTs [45].

In this work, F-implanted buried layer (FIBL) has been introduced underneath p-NiO in the termination region, which can effectively suppress the p-NiO-induced reverse leakage. The leakage mechanisms in vertical GaN SBD with p-NiO JTE have been investigated by photon emission microscopy (PEM) measurements and electrical characterizations, whereby the role of FIBL in suppressing the leakage current in p-NiO JTE has been identified. Thanks to the hybrid p-NiO JTE (HP-JTE) with FIBL as well as the nearly ideal Schottky interface, the vertical GaN SBD exhibits a high current swing of ∼10^{13}, a low ideality factor of ∼1.02, a low differential R_{ON} of ∼0.89 mΩ · cm^2, a low forward voltage drop (V_F) of ∼0.8 V (defined at 100 A/cm^2), and a breakdown voltage of ∼780 V (defined at 0.1 A/cm^2).

II. DEVICE STRUCTURE AND FABRICATION

Fig. 1 shows the schematic cross-section and the key fabrication process steps of the vertical GaN SBD with HP-JTE. 1.4 μm-thick SiO_2 was deposited by plasma-enhanced chemical vapor deposition (PECVD) and patterned to form the hard mask for selective-area F ion implantation. Multi-energy F ion implantation with energy levels of 30, 60 and 100 keV at doses of 5×10^{12}, 1.5×10^{13} and 3×10^{13} cm^{-2} were carried out to form F-implanted region. For recovery of the possible implantation-induced damage, post-implantation annealing (PIA) was performed at 450 °C in N_2 ambient for 20 minutes, with the sample surface covered by a

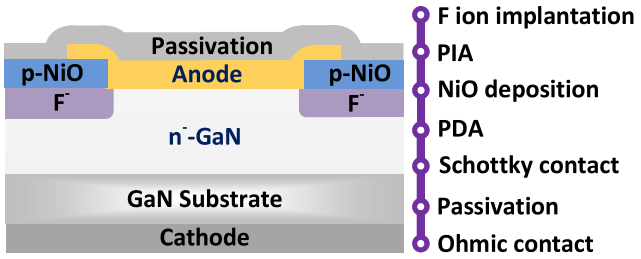

FIGURE 1. Schematic cross-section and the key fabrication process steps of the vertical GaN SBD with HP-JTE

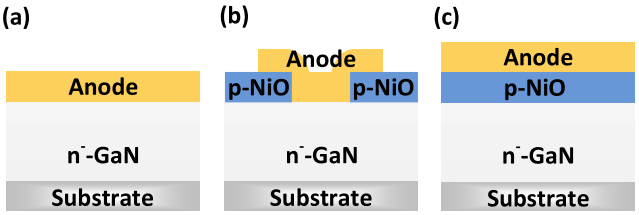

FIGURE 2. Schematic cross-sections of (a) unterminated-SBD, (b) SBD with p-NiO JTE and (c) p-NiO/n-GaN HJ diode with a uniform p-NiO layer in the anode region

pre-deposited SiO_2 protection layer. After the removal of SiO_2 protection layer, ∼200 nm p-type NiO was deposited by magnetron sputtering with a O_2/(Ar+O_2) flux ratio of ∼5% [31], followed by lift-off process to form p-NiO JTE. Post-deposition annealing (PDA) was carried out at 300 °C in N_2 ambient for 5 minutes to reduce the p-NiO-induced leakage current [35]. Afterwards, Ni/Au anode metal stack was deposited on the pre-cleaned GaN surface and patterned by lift-off. ∼200 nm SiO_2 passivation layer was deposited, followed by via hole opening. Finally, ohmic contact on the n$^+$-GaN substrate was formed by deposition of Ti/Al/Ti/Au metal stack. Meanwhile, unterminated-SBD (Fig. 2(a)), SBD with p-NiO JTE (Fig. 2(b)) and p-NiO/n-GaN HJ diode with a uniform p-NiO layer in the anode region (Fig. 2 (c)) were also fabricated on the same wafer for comparison.

III. RESULTS AND DISCUSSIONS

Capacitance–voltage (C-V) measurement was carried out to extract the net doping concentration in the 10 μm-thick n$^-$-GaN drift layer, which is ∼8×10^{15} cm^{-3}, as shown in Fig. 3. Fig. 4(a) shows the forward I-V characteristics and the ideality factor of the vertical GaN SBD with HP-JTE. The near-unity ideality factor (∼1.02) in the barrier-limited region, low intrinsic leakage current of ∼10^{-10} A/cm^2 and high current swing up to ∼10^{13} suggest the nearly ideal Schottky interface and high-quality GaN-on-GaN homo-epitaxial layer, with thermionic emission (TE) as the dominant carrier transport mechanism at forward bias [41], [46]. As shown in Fig. 4(b), the vertical GaN SBD with HP-JTE exhibits a low differential R_{ON} of ∼0.89 mΩ · cm^2 that saturates at ∼1 V (Fig. 4(b)). Owing to the relatively low Schottky barrier height at Ni/n$^-$-GaN as

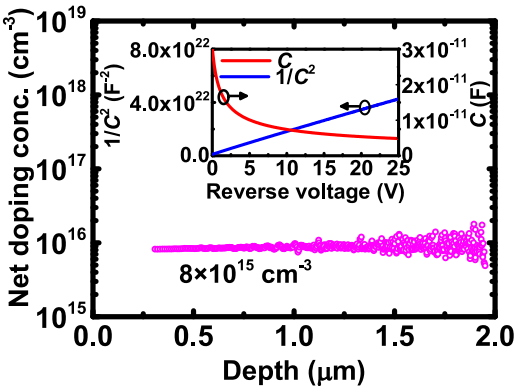

FIGURE 3. Net doping concentration of the n$^-$ GaN drift layer. Inset: measured *C-V* and $1/C^2$-*V* characteristics.

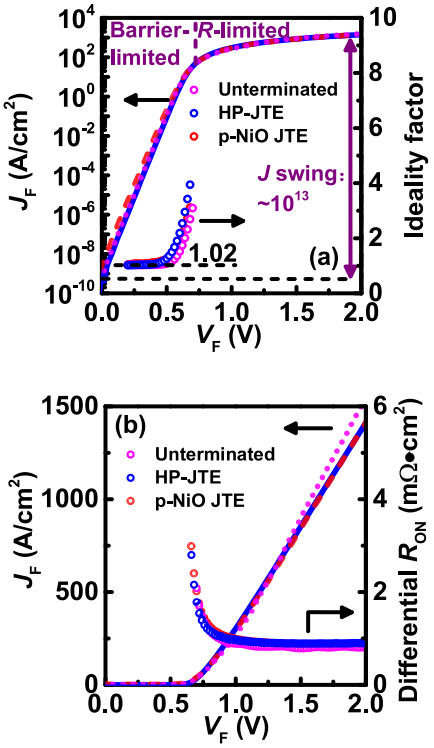

FIGURE 4. (a) Forward *I-V* characteristics and ideality factor versus forward voltage in semi-log scale, (b) forward *I-V* characteristics and differential R_{ON} versus forward voltage in linear-scale of the vertical GaN SBD with HP-JTE, SBD with p-NiO JTE and unterminated SBD.

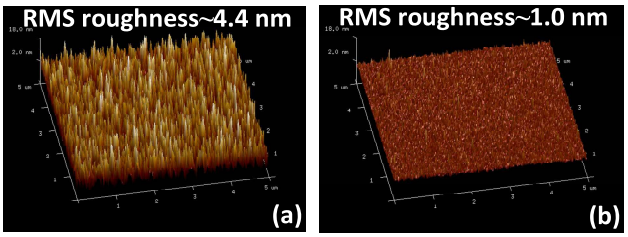

FIGURE 5. AFM images of p-NiO surface (a) before and (b) after PDA.

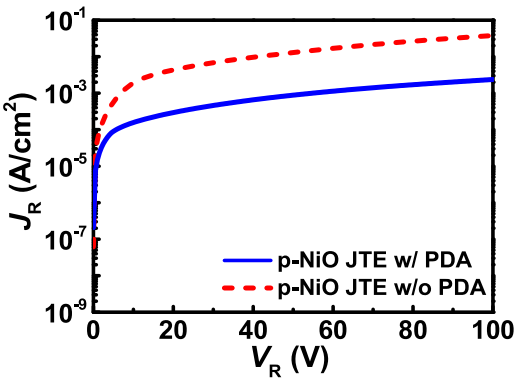

FIGURE 6. Reverse *I-V* characteristics of the SBDs featuring p-NiO JTE with and without PDA.

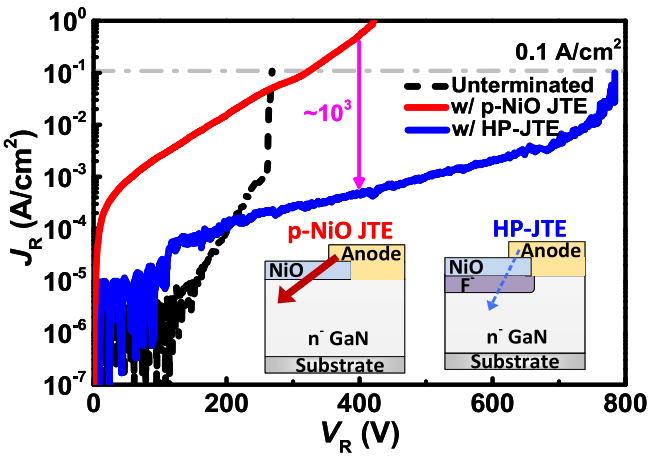

FIGURE 7. Reverse *I-V* characteristics of unterminated SBD, SBD with p-NiO JTE, and SBD with HP-JTE. Inset: Illustration of the possible main leakage paths in SBDs with p-NiO JTE and HP-JTE.

well as the sharp turn-on transition, a low V_F (defined at 100 A/cm^2) of ~0.8 V was obtained (Fig. 4(b)). The forward conduction characteristics of SBD with p-NiO JTE and unterminated SBD are also shown in Fig. 4. Similarly, the GaN SBD with p-NiO JTE and unterminated SBD also exhibit a high current swing up to ~10^{13}, a near-unity ideality factor and a low V_F of ~0.8 V, benefiting from the optimal Schottky interface and high-quality GaN-on-GaN homo-epitaxial layer. The unterminated SBD exhibits a slightly lower differential R_{ON} of ~0.80 mΩ·cm^2, due to the absence of the overlap between anode metal and termination region as in SBDs with HP-JTE and p-NiO JTE.

The influence of the PDA on the surface morphology and leakage current of p-NiO have been investigated. According to the atomic force microscope (AFM) measurements (Fig. 5), the PDA following p-NiO deposition can reduce the root-mean-square (RMS) roughness of p-NiO surface from ~4.4 nm to ~1.0 nm. The reverse leakage characteristics of vertical GaN SBDs featuring p-NiO JTE with and without PDA are compared in Fig. 6. PDA after p-NiO deposition can effectively reduce the leakage current, which is possibly due to the improved p-NiO/GaN interface [35] or the

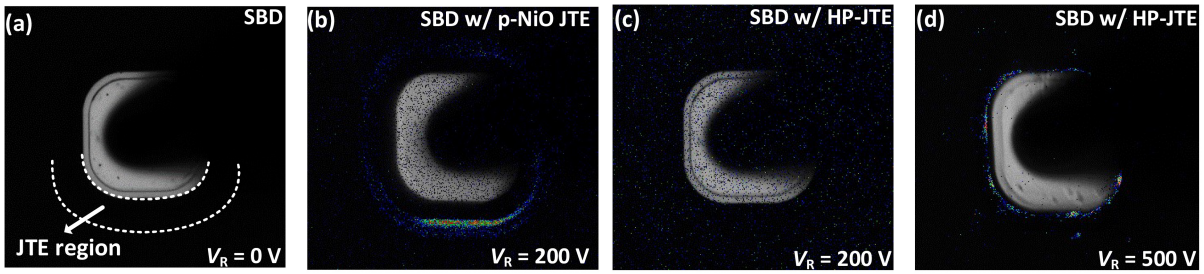

FIGURE 8. PEM images of (a) SBDs at 0 V, (b) SBD with p-NiO JTE at reverse voltage (V_R) of 200 V, (c) SBD with HP-JTE at V_R of 200 V, (d) SBD with HP-JTE at V_R of 500 V. The anode metal is opaque.

decreased Ni^{3+} composition in p-NiO according to the X-ray photoelectron spectroscopy (XPS) measurements [47]. In order to further reduce the leakage current, it is significant to reveal the possible leakage paths in SBD with p-NiO JTE and develop effective leakage suppression approaches.

There could be two possible leakage paths in SBD with p-NiO JTE: 1) anode region leakage through the metal/n^--GaN Schottky contact particularly with barrier lowering effect at high electric field [48] or with considerable traps [49], [50]; 2) termination region leakage through p-NiO or through the p-NiO/GaN interface. The reverse leakage characteristics of the SBD with HP-JTE (Fig. 1), unterminated-SBD (Fig. 2(a)), and SBD with p-NiO JTE (Fig. 2 (b)) are compared in Fig. 7. Benefiting from the nearly ideal Schottky interface and superior quality of n^--GaN drift layer, unterminated-SBD shows a relatively low leakage current under reverse voltage of 100 V, suggesting the possible anode region leakage through the metal/n^--GaN Schottky contact is insignificant at relatively low reverse voltage. Compared with unterminated-SBD, SBD with p-NiO JTE shows relatively high leakage currents, which could verify that the termination region leakage through p-NiO or through the p-NiO/GaN interface is possibly dominated in SBD with p-NiO JTE.

In order to suppress the leakage current induced by p-NiO, FIBL was formed underneath p-NiO in the JTE regions (Fig. 1). Compared with SBD with p-NiO JTE only, the leakage current of SBD with HP-JTE is reduced by approximately 3 orders of magnitude under reverse voltage of ~400 V and enables a breakdown voltage of ~780 V (defined at leakage current of 0.1 A/cm^2), as shown in Fig. 7.

PEM has been widely acknowledged as a useful approach to localizing the regions with relatively high leakage current in electronic devices [51], [52]. In this work, to reveal the influence of FIBL on the leakage current in p-NiO region, PEM measurements were carried out with an optical test system (P-100I) featuring spectral sensitivity from 300 nm to 1700 nm. At 0 V, there is no light emission detected in the SBDs, as shown in Fig. 8(a). Fig. 8(b) and Fig. 8(c) show the PEM images of SBD with p-NiO JTE and SBD with HP-JTE at a reverse voltage of 200 V, respectively. In comparison with the stronger light emission from the p-NiO region in the SBD with p-NiO JTE only, there is no detectable light emission in SBD with HP-JTE at a reverse voltage of 200 V, suggesting that the leakage current through p-NiO has been effectively suppressed by FIBL. At higher reverse voltage of 500 V, light emission was detected in the SBD with HP-JTE, as shown in Fig. 8(d).

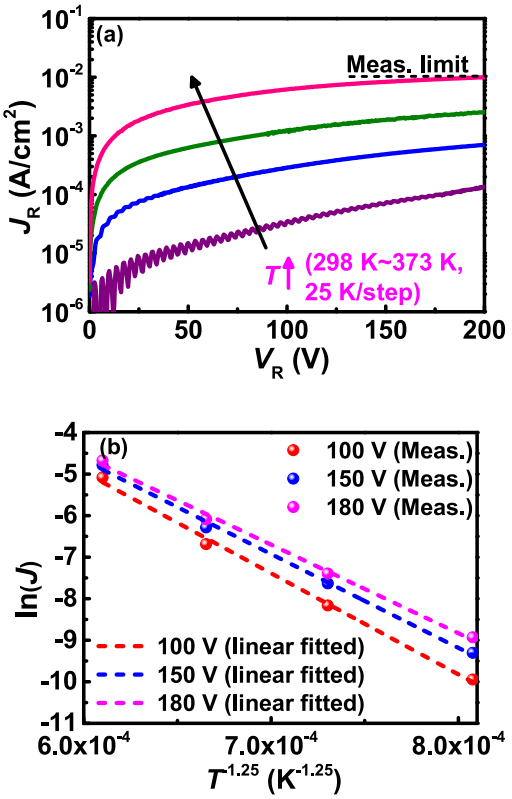

FIGURE 9. (a) Temperature-dependent reverse I-V characteristics and (b) ln(J) versus $T^{-1.25}$ characteristics of the p-NiO/n^--GaN HJ diode.

The possible leakage mechanism of the p-NiO/n^--GaN hetero-junction was also investigated. Fig. 9(a) shows the reverse current characteristics of the p-NiO/n^--GaN HJ diode at temperatures varying from 298 K to 373 K. Temperature- and field-enhanced variable-range hopping (VRH) conduction [15], [50], [53], [54], [55] could be responsible for the leakage of the p-NiO/n^--GaN hetero-junction. In VRH model, the leakage current density J can be described by

$$J = J_0 \exp\left(C\frac{qaE}{2kT}\left(\frac{T_0}{T}\right)^{\frac{1}{4}}\right) \quad (1)$$

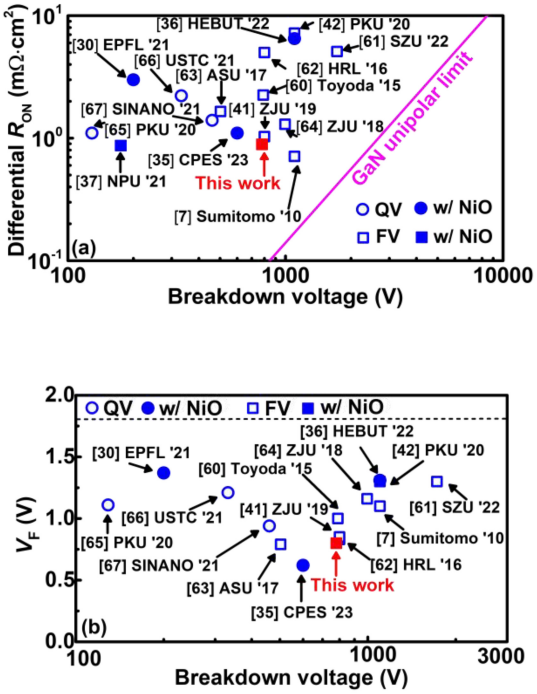

FIGURE 10. **(a) Benchmark of differential R_{ON} versus breakdown voltage (defined at 0.1 A/cm^2) and (b) benchmark of V_F (defined at 100 A/cm^2) versus breakdown voltage for the state-of-the-art fully-vertical (FV) and quasi-vertical (QV) GaN SBDs. The reported SBDs with NiO-based termination technology are particularly denoted with solid symbols.**

where J_0 is the zero-field current density, C is a constant multiplication factor, q is the elementary charge, a is the localization radius of the electron wave function, k is the Boltzmann's constant, E is electrical field, T is temperature, T_0 is a characteristic temperature which is determined by the energy barrier between two adjacent localized states for electron hopping, as well as the density of localized states at the Fermi level [54], [55]. Fig. 9(b) shows the relationship between ln(J) and $T^{-1.25}$ at various reverse biases. It is found that there is a linear correlation between ln(J) and $T^{-1.25}$ at various reverse biases, suggesting that the leakage current of p-NiO/n$^-$-GaN hetero-junction is primarily dominated by VRH mechanism. It has been reported that there exist defect-induced trap levels within the bandgap of NiO according to photoluminescence spectroscopy [56] and X-ray photoelectron spectroscopy [57] measurements, which could possibly lead to VRH leakage through p-NiO/n$^-$-GaN hetero-junction. In particular, it has been identified that the p-type conductivity in NiO is most likely associated with Ni vacancies, according to X-ray absorption spectroscopy measurements [58], [59]. The defect-assisted conduction/leakage could possibly present long-term reliability issues, which merit further in-depth investigations in future work.

Fig. 10(a) shows the benchmark of differential R_{ON} versus breakdown voltage (defined at 0.1 A/cm^2) and Fig. 10(b) shows the benchmark of V_F (defined at 100 A/cm^2) versus breakdown voltage (defined at 0.1 A/cm^2) of the state-of-the-art quasi-vertical and fully-vertical GaN SBDs. The SBD with HP-JTE in this work exhibits a low differential R_{ON} (∼0.89 mΩ·cm^2) and a low V_F (∼0.8 V), yielding a BFOM of ∼0.68 GW/cm^2 that is competitive among the reported GaN SBDs with p-NiO-based termination.

IV. CONCLUSION

In this work, we demonstrate a vertical GaN SBD featuring hybrid p-NiO JTE (HP-JTE) with fluorine-implanted buried layer (FIBL). With FIBL incorporated underneath p-NiO in the termination region, the reverse leakage current can be effectively reduced by approximately 3 orders of magnitude. According to light emission in PEM measurements, it has also been verified that the leakage through p-NiO in termination region can be effectively suppressed by FIBL. Thanks to the HP-JTE structure as well as the nearly ideal Schottky interface, the vertical GaN SBD exhibits a high current swing of ∼10^{13}, a low ideality factor of ∼1.02, a low differential R_{ON} of ∼0.89 mΩ · cm^2, a low forward voltage drop of ∼0.8 V (defined at 100 A/cm^2), and a breakdown voltage of ∼780 V (defined at 0.1 A/cm^2). In addition, it has been found that the annealing process following p-NiO deposition can reduce surface roughness of p-NiO as well as the leakage current. According to temperature-dependent electrical characterizations, the leakage current in the p-NiO/n$^-$-GaN hetero-junction is possibly dominated by the temperature- and field-enhanced variable-range hopping (VRH) conduction mechanism. The characterizations and findings in this work can provide valuable insights into the p-NiO/GaN hetero-junction-based power devices.

REFERENCES

[1] K. J. Chen et al., "GaN-on-Si power technology: Devices and applications," *IEEE Trans. Electron Devices*, vol. 64, no. 3, pp. 779–795, Mar. 2017, doi: 10.1109/TED.2017.2657579.

[2] Y. Zhang, F. Udrea, and H. Wang, "Multidimensional device architectures for efficient power electronics," *Nat. Electron.*, vol. 5, no. 11, pp. 723–734, Nov. 2022, doi: 10.1038/s41928-022-00860-5.

[3] (Toyoda Gosei Co., Aichi, Japan). *Toyoda Gosei Succeeds in Making Larger GaN Substrates for Next-Generation Power Devices*. Mar. 15, 2022. [Online]. Available: https://www.toyodagosei.com/News/1335/toyoda-gosei-succeeds-in-making-larger-gan-substrates-for-next-generation-power

[4] V. Talesara, Y. Zhang, V. Gopal, T. Vangipuram, H. Zhao, and W. Lu, "Vertical GaN-on-GaN pn power diodes with Baliga figure of merit of 27 GW/cm^2," *Appl. Phys. Lett.*, vol. 122, no. 12, Mar. 2023, Art. no. 123501, doi: 10.1063/5.0135313.

[5] K. Nomoto et al., "GaN-on-GaN p-n power diodes with 3.48 kV and 0.95 mΩ · *cm*^{2}: A record high figure-of-merit of 12.8 GW/cm^2," in *Proc. IEEE Int. Electron Devices Meeting (IEDM)*, 2015, pp. 9.7.1–9.7.4, doi: 10.1109/IEDM.2015.7409665.

[6] H. Ohta, K. Hayashi, F. Horikiri, M. Yoshino, T. Nakamura, and T. Mishima, "5.0 kV breakdown-voltage vertical GaN p–n junction diodes," *Jpn. J. Appl. Phys.*, vol. 57, no. 4, Feb. 2018, Art. no. 4FG09, doi: 10.7567/JJAP.57.04FG09.

[7] Y. Saitoh et al., "Extremely low on-resistance and high breakdown voltage observed in vertical GaN Schottky barrier diodes with high-mobility drift layers on low-dislocation-density GaN substrates," *Appl. Phys. Exp.*, vol. 3, no. 8, Jul. 2010, Art. no. 81001, doi: 10.1143/APEX.3.081001.

[8] X. Liu et al., "Vertical GaN Schottky barrier diode with record high figure of merit (1.1 GW/cm^2) fully grown by hydride vapor phase epitaxy," *IEEE Trans. Electron Devices*, vol. 70, no. 7, pp. 3748–3753, Jul. 2023, doi: 10.1109/TED.2023.3279059.

[9] S. Han, S. Yang, R. Li, X. Wu, and K. Sheng, "Current-collapse-free and fast reverse recovery performance in vertical GaN-on-GaN Schottky barrier diode," *IEEE Trans. Power Electron.*, vol. 34, no. 6, pp. 5012–5018, Jun. 2019, doi: 10.1109/TPEL.2018.2876444.

[10] A. D. Koehler et al., "Vertical GaN junction barrier Schottky diodes," *ECS J. Solid State Sci. Technol.*, vol. 6, no. 1, pp. Q10–Q12, Jan. 2017, doi: 10.1149/2.0041701jss.

[11] F. Zhou et al., "High-voltage quasi-vertical GaN junction barrier Schottky diode with fast switching characteristics," *IEEE Electron Device Lett.*, vol. 42, no. 7, pp. 974–977, Jul. 2021, doi: 10.1109/LED.2021.3078477.

[12] Y. Zhang et al., "Vertical GaN junction barrier Schottky rectifiers by selective ion implantation," *IEEE Electron Device Lett.*, vol. 38, no. 8, pp. 1097–1100, Aug. 2017, doi: 10.1109/LED.2017.2720689.

[13] M. Matys, K. Kitagawa, T. Narita, T. Uesugi, J. Suda, and T. Kachi, "Mg-implanted vertical GaN junction barrier Schottky rectifiers with low on resistance, low turn-on voltage, and nearly ideal nondestructive breakdown voltage," *Appl. Phys. Lett.*, vol. 121, no. 20, p. 3507, Nov. 2022, doi: 10.1063/5.0106321.

[14] S. R. Stein et al., "Analysis of vertical GaN JBS and p-n diodes by Mg ion implantation and ultrahigh-pressure annealing," *IEEE Trans. Electron Devices*, vol. 71, no. 3, pp. 1494–1501, Mar. 2024, doi: 10.1109/TED.2023.3339592.

[15] Z. Hu et al., "1.1-kV vertical GaN p-n diodes with p-GaN regrown by molecular beam epitaxy," *IEEE Electron Device Lett.*, vol. 38, no. 8, pp. 1071–1074, Aug. 2017, doi: 10.1109/LED.2017.2720747.

[16] K. Fu et al., "Demonstration of 1.27 kV etch-then-regrow GaN p–n junctions with low leakage for GaN power electronics," *IEEE Electron Device Lett.*, vol. 40, no. 11, pp. 1728–1731, Nov. 2019, doi: 10.1109/LED.2019.2941830.

[17] T. Narita, T. Kachi, K. Kataoka, and T. Uesugi, "P-type doping of GaN by magnesium ion implantation," *Appl. Phys. Express*, vol. 10, Dec. 2016, Art. no. 16501, doi: 10.7567/APEX.10.016501.

[18] H. Sakurai et al., "Highly effective activation of Mg-implanted p-type GaN by ultra-high-pressure annealing," *Appl. Phys. Lett.*, vol. 115, no. 14, Sep. 2019, Art. no. 142104, doi: 10.1063/1.5116866.

[19] M. H. Breckenridge et al., "High Mg activation in implanted GaN by high temperature and ultrahigh pressure annealing," *Appl. Phys. Lett.* vol. 118, no. 2, Jan. 2021, Art. no. 22101, doi: 10.1063/5.0038628.

[20] J. D. Greenlee, B. N. Feigelson, T. J. Anderson, J. K. Hite, K. D. Hobart, and F. J. Kub, "Symmetric multicycle rapid thermal annealing: Enhanced activation of implanted dopants in GaN," *ECS J. Solid State Sci. Technol.*, vol. 4, no. 9, pp. P382–P386, Aug. 2015, doi: 10.1149/2.0191509jss.

[21] S. Kotzea, A. Debald, M. Heuken, H. Kalisch, and A. Vescan, "Demonstration of a GaN-based vertical-channel JFET fabricated by selective-area regrowth," *IEEE Trans. Electron Devices*, vol. 65, no. 12, pp. 5329–5336, Dec. 2018, doi: 10.1109/TED.2018.2875534.

[22] M. Xiao et al., "Origin of leakage current in vertical GaN devices with nonplanar regrown p-GaN," *Appl. Phys. Lett.*, vol. 117, no. 18, Nov. 2020, Art. no. 183502, doi: 10.1063/5.0021374.

[23] A. S. Chang et al., "Unveiling the influence of selective-area-regrowth interfaces on local electronic properties of GaN p-n junctions for efficient power devices," *Nano Energy*, vol. 102, no. 2, Nov. 2022, Art. no. 107689, doi: 10.1016/j.nanoen.2022.107689.

[24] M. Monavarian et al., "High-voltage regrown nonpolar m-plane vertical p-n diodes: A step toward future selective-area-doped power switches," *IEEE Electron Device Lett.*, vol. 40, no. 3, pp. 387–390, Mar. 2019, doi: 10.1109/LED.2019.2892345.

[25] G. W. Pickrell et al., "Investigation of dry-etch-induced defects in >600 V regrown vertical GaN p-n diodes using deep-level optical spectroscopy," *J. Appl. Phys.*, vol. 126, no. 14, Oct. 2019, Art. no. 145703, doi: 10.1063/1.5110521.

[26] T. Zhang, L. Liuan, and A. Jin-Ping, "Temperature-dependent electrical transport characteristics of a NiO/GaN heterojunction diode," *Surfaces Interfaces*, vol. 5, pp. 15–18, Dec. 2016, doi: 10.1016/j.surfin.2016.08.004.

[27] M. Xiao et al., "First demonstration of vertical superjunction diode in GaN," in *Proc. IEDM*, 2022, pp. 35.6.1–35.6.4, doi: 10.1109/IEDM45625.2022.10019405.

[28] K. Baraik et al., "Epitaxial growth and band alignment properties of NiO/GaN heterojunction for light emitting diode applications," *Appl. Phys. Lett.*, vol. 110, no. 19, May 2017, Art. no. 191603, doi: 10.1063/1.4983200.

[29] M. D. Irwin, D. B. Buchholz, A. W. Hains, R. P. H. Chang, and T. J. Marks, "p-Type semiconducting nickel oxide as an efficiency-enhancing anode interfacial layer in polymer bulk-heterojunction solar cells," *Proc. Nat. Acad. Sci. USA*, vol. 105, pp. 2783–2787, Feb. 2008, doi: 10.1073/pnas.0711990105.

[30] R. A. Khadar et al., "p-NiO junction termination extensions for high voltage vertical GaN devices, in *Proc. 33rd Int. Symp. Power Semicond. Devices ICs (ISPSD)*, 2021, pp. 147–150, doi: 10.23919/ISPSD50666.2021.9452255.

[31] W. Hao et al.,"Improved vertical β-Ga_2O_3 Schottky barrier diodes with conductivity-modulated p-NiO junction termination extension," *IEEE Trans. Electron Devices*, vol. 70, no. 4, pp. 2129–2134, Apr. 2023, doi: 10.1109/TED.2023.3241885.

[32] Y. Ren et al., "Quasi-vertical GaN heterojunction diodes with p-NiO anodes deposited by sputtering and post-annealing," *Vacuum*, vol. 182, Dec. 2020, Art. no. 109784, doi: 10.1016/j.vacuum.2020.109784.

[33] S. J. Huang et al., "Achievement of normally-off AlGaN/GaN high-electron mobility transistor with p-NiO_x capping layer by sputtering and post-annealing," *Appl. Surf. Sci.*, vol. 401, pp. 373–377, Apr. 2017, doi: 10.1016/j.apsusc.2017.01.032.

[34] H. Guo et al., "Over 1200 V normally-OFF p-NiO gated AlGaN/GaN HEMTs on Si with a small threshold voltage shift," *IEEE Electron Device Lett.*, vol. 43, no. 2, pp. 268–271, Feb. 2022, doi: 10.1109/LED.2021.3137510.

[35] Y. Qin et al., "1 kV GaN-on-Si quasi-vertical Schottky rectifier," *IEEE Electron Device Lett.*, vol. 44, no. 7, pp. 1052–1055, Jul. 2023, doi: 10.1109/LED.2023.3282025.

[36] F. Huang et al., "GaN-based quasi-vertical Schottky barrier diode hybridized with p-NiO layer to achieve 1.1 kV breakdown voltage and enhance the current spreading effect," *Appl. Phys. Express*, vol. 15, no. 8, Jul. 2022, Art. no. 84001, doi: 10.35848/1882-0786/ac7eac.

[37] Y. Wang, T. Pu, X. Li, L. Li, and J.-P. Ao, "Application of p-type NiO deposited by magnetron reactive sputtering on GaN vertical diodes," *Mater. Sci. Semicond. Process.*, vol. 125, Apr. 2021, Art. no. 105628, doi: 10.1016/j.mssp.2020.105628.

[38] J. Zhou, L. He, X. Li, T. Pu, L. Li, and J.-P. Ao, "Vertical GaN Schottky barrier diodes with area-selectively deposited p-NiO guard ring termination structure," *Superlattices Microstructures*, vol. 151, Mar. 2021, Art. no. 106820, doi: 10.1016/j.spmi.2021.106820.

[39] M. Wang, L. Yuan, C. C. Cheng, C. D. Beling, and K. J. Chen, "Defect formation and annealing behaviors of fluorine-implanted GaN layers revealed by positron annihilation spectroscopy," *Appl. Phys. Lett.*, vol. 94, no. 6, Feb. 2009, Art. no. 61910, doi: 10.1063/1.3081019.

[40] M. Wang, C. C. Cheng, C. D. Beling, S. Fung, and K. J. Chen, "Modulation of polarization field by fluorine ions in AlGaN/GaN heterostructures revealed by positron annihilation spectroscopy," *Phys. Status Solidi A*, vol. 207, no. 6, pp. 1332–1334, May 2010, doi: 10.1002/pssa.200983463.

[41] S. Han, S. Yang, and K. Sheng, "Fluorine-implanted termination for vertical GaN Schottky rectifier with high blocking voltage and low forward voltage drop," *IEEE Electron Device Lett.*, vol. 40, no. 7, pp. 1040–1043, Jul. 2019, doi: 10.1109/LED.2019.2915578.

[42] R. Yin et al., "High voltage vertical GaN-on-GaN Schottky barrier diode with high energy fluorine ion implantation based on space charge induced field modulation (SCIFM) effect," in *Proc. 32nd Int. Symp. Power Semicond. Devices ICs (ISPSD)*, 2020, pp. 298–301, doi: 10.1109/ISPSD46842.2020.9170190.

[43] Z. Liu et al., "High-voltage vertical GaN-on-GaN Schottky barrier diode using fluorine ion implantation treatment," *AIP Adv.*, vol. 9, no. 5, 2019, Art. no. 55016, doi: 10.1063/1.5100251.

[44] J. Chen et al., "A GaN-on-Si quasi-vertical Schottky barrier diode with enhanced performance using fluorine ion-implanted field rings," *Appl. Phys. Exp.*, vol. 14, no. 11, Nov. 2021, Art. no. 116504, doi: 10.35848/1882-0786/ac2e9c.

[45] S. Yang, S. Huang, M. Schnee, Q.-T. Zhao, J. Schubert, and K. J. Chen, "Fabrication and characterization of enhancement-mode high-k $LaLuO_3$-AlGaN/GaN MIS-HEMTs," *IEEE Trans. Electron Devices*, vol. 60, no. 10, pp. 3040–3046, Oct. 2013, doi: 10.1109/TED.2013.2277559.

[46] S. Yang, S. Han, and K. Sheng, "Vertical GaN power rectifiers: Interface effects and switching performance," *Semicond. Sci. Technol.*, vol. 36, no. 2, Dec. 2020, Art. no. 24005, doi: 10.1088/1361-6641/abca0d.

[47] W. Hao et al., "Low defect density and small *I–V* curve hysteresis in NiO/β-Ga2O3 pn diode with a high PFOM of 0.65 GW/cm^2," *Appl. Phys. Lett.*, vol. 118, no. 4, Jan. 2021, Art. no. 43501, doi: 10.1063/5.0038349.

[48] T. Hatakeyama and T. Shinohe, "Reverse characteristics of a 4H-SiC Schottky barrier diode," *Mater. Sci. Forum*, vols. 389–393, pp. 1169–1172, Apr. 2002, doi: 10.4028/www.scientific.net/MSF.389-393.1169.

[49] J. Miller, E. T. Yu, P. Waltereit, and J. S. Speck, "Analysis of reverse-bias leakage current mechanisms in GaN grown by molecular-beam epitaxy," *Appl. Phys. Lett.*, vol. 84, no. 4, pp. 535–537, Jan. 2004.

[50] J. Chen et al., "Determination of the leakage current transport mechanisms in quasi-vertical GaN–on–Si Schottky barrier diodes (SBDs) at low and high reverse biases and varied temperatures," *Appl. Phys. Exp.*, vol. 14, no. 10, Oct. 2021, Art. no. 104002, doi: 10.35848/1882-0786/ac2260.

[51] I. D. Wolf and M. Rasras, "Spectroscopic photon emission microscopy: A unique tool for failure analysis of microelectronics devices," *Microelectron. Reliab.*, vol. 41, no. 8, pp. 1161–1169, Aug. 2001, doi: 10.1016/S0026-2714(01)00104-4.

[52] J. C. H. Phang et al., "A review of near infrared photon emission microscopy and spectroscopy," in *Proc. 12th Int. Symp. Phys. Failure Anal. Integr. Circuits (IPFA)*, 2005, pp. 275–281, doi: 10.1109/IPFA.2005.1469178.

[53] D. V. Kuksenkov, H. Temkin, A. Osinsky, R. Gaska, and M. A. Khan, "Origin of conductivity and low-frequency noise in reverse-biased GaN p-n junction," *Appl. Phys. Lett.*, vol. 72, no. 11, pp. 1365–1367, Mar. 1998, doi: doi.org/10.1063/1.121056.

[54] J. Liu, C. Han, W. Liu, L. Geng, and Y. Hao, "Leakage reduction of quasi-vertical GaN Schottky barrier diode with post oxygen plasma treatment," *IEEE Trans. Electron Devices*, vol. 69, no. 12, pp. 6929–6933, Dec. 2022, doi: 10.1109/TED.2022.3212336.

[55] Y. X. Lin et al., "Ultra-low turn-on voltage quasi-vertical GaN Schottky barrier diode with homogeneous barrier height," *Solid State Electron.*, vol. 207, Sep. 2023, Art. no. 108723, doi: 10.1016/j.sse.2023.108723.

[56] S. Mochizuki and T. Saito, "Intrinsic and defect-related luminescence of NiO," *Phys. B, Condens. Matter*, vol. 404, nos. 23–24, pp.4850–4853, Dec. 2009, doi: 10.1016/j.physb.2009.08.166.

[57] K. O. Egbo, C. P. Liu, C. E. Ekuma, and K. M. Yu, "Vacancy defects induced changes in the electronic and optical properties of NiO studied by spectroscopic ellipsometry and first-principles calculations," *J. Appl. Phys.*, vol. 128, no. 13, Oct. 2020, Art. no. 135705, doi: 10.1063/5.0021650.

[58] W.-L. Jang, Y.-M. Lu, W.-S. Hwang, T.-L. Hsiung, and H. P. Wang, "Point defects in sputtered NiO films," *Appl. Phys. Lett.*, vol. 94, no. 6, Feb. 2009, Art. no. 62103, doi: 10.1063/1.3081025.

[59] D.-Y. Cho, S. J. Song, U. K. Kim, K. M. Kim, H.-K. Lee, and C. S. Hwang, "Spectroscopic investigation of the hole states in Ni-deficient NiO films," *J. Mater. Chem. C*, vol. 1, no. 28, pp. 4334–4338, May, 2013, doi: 10.1039/c3tc30687a.

[60] N. Tanaka, K. Hasegawa, K. Yasunishi, N. Murakami, and T. Oka, "50 A vertical GaN Schottky barrier diode on a free-standing GaN substrate with blocking voltage of 790 V," *Appl. Phys. Exp.*, vol. 8, no. 7, Jul. 2015, Art. no. 71001. doi: 10.7567/APEX.8.071001.

[61] X. Liu et al., "1.7-kV vertical GaN-on-GaN Schottky barrier diodes with helium-implanted edge termination," *IEEE Trans. Electron Devices*, vol. 69, no. 4, pp. 1938–1944, Apr. 2022, doi: 10.1109/TED.2022.3153594.

[62] Y. Cao, R. Chu, R. Li, M. Chen, R. Chang, and B. Hughes, "High-voltage vertical GaN Schottky diode enabled by low-carbon metal-organic chemical vapor deposition growth," *Appl. Phys. Lett.*, vol. 108, no. 6, Feb. 2016, Art. no. 62103, doi: 10.1063/1.4941814.

[63] H. Fu, X. Huang, H. Chen, Z. Lu, I. Baranowski, and Y. Zhao, "Ultra-low turn-on voltage and on-resistance vertical GaN-on-GaN Schottky power diodes with high mobility double drift layers," *Appl. Phys. Lett.*, vol. 111, no. 15, Oct. 2017, Art. no. 152102, doi: 10.1063/1.4993201.

[64] S. Han, S. Yang, and K. Sheng, "High-voltage and high-I_{ON}/I_{OFF} vertical GaN-on-GaN Schottky barrier diode with nitridation-based termination," *IEEE Electron Device Lett.*, vol. 39, no. 4, pp. 572–575, Apr. 2018, doi: 10.1109/LED.2018.2808684.

[65] Y. Li et al., "Quasi-vertical GaN Schottky barrier diode on silicon substrate with 10^{10} high on/off current ratio and low specific on-resistance," *IEEE Electron Device Lett.*, vol. 41, no. 3, pp. 329–332, Mar. 2020, doi: 10.1109/LED.2020.2968392.

[66] X. Guo et al., "High-voltage and high-I_{ON}/I_{OFF} quasi-vertical GaN-on-Si Schottky barrier diode with argon-implanted termination," *IEEE Electron Device Lett.*, vol. 42, no. 4, pp. 473–476, Apr. 2021, doi: 10.1109/LED.2021.3058380.

[67] X. Guo et al., "Nitrogen-implanted guard rings for 600-V quasi-vertical GaN-on-Si Schottky barrier diodes with a BFOM of 0.26 GW/cm^2," *IEEE Trans. Electron Devices*, vol. 68, no. 11, pp. 5682–5686, Nov. 2021, doi: 10.1109/TED.2021.3108951.